THE JOURNAL OF PHYSICAL CHEMISTRY B

ARTICLE

pubs.acs.org/JPCB

# Cooperativity in Long $\alpha$- and $3_{10}$-Helical Polyalanines: Both Electrostatic and van der Waals Interactions Are Essential

Shugui Hua, Lina Xu, Wei Li, and Shuhua Li*

School of Chemistry and Chemical Engineering, Key Laboratory of Mesoscopic Chemistry of MOE, Institute of Theoretical and Computational Chemistry, Nanjing University, Nanjing 210093, P. R. China

Supporting Information

**ABSTRACT:** We have employed the generalized energy-based fragmentation (GEBF) approach to investigate the structures, energies, and enthalpies of $\alpha$-helices, $3_{10}$-helices, and $\beta$-strands for capped polyalanines, acetyl(ala)$_N$NH$_2$, with $N$ values from 8 to 40 at several theoretical levels. The M06-2X functional is demonstrated to be much more accurate than the B3LYP functional for peptides under study. On the basis of the GEBF-M06-2X results, we find that $\alpha$-helices are more stable than the corresponding $3_{10}$-helices for all peptides with $N \geq 10$. The cooperative interaction in both helices have not reached their asymptotic limits even for $N = 40$. By comparing the performance of the M06-2X, B3LYP, and the van der Waals corrected B3LYP, we show that both electrostatic and van der Waals interactions are essential for describing the cooperative interaction in long helices. In addition, the greater cooperativity of $\alpha$-helices over $3_{10}$-helices in long helices is found to originate mainly from the much stronger van der Waals interaction in $\alpha$-helices.

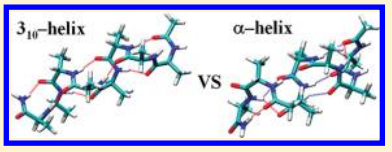


## 1. INTRODUCTION

In protein structures, most of the residues are found in locally regular conformations such as helices, sheets, and turns.[1] Among secondary structures, the helix is the most abundant structural motif in proteins. Depending on the hydrogen bonds (HBs) formed between amino acid residues, helices can be divided into two main types, $3_{10}$-helix and $\alpha$-helix. The former corresponds to the HB between residues $i$ and $i + 3$, and the latter corresponds to the HB between $i$ and $i + 4$, respectively. Understanding the factors that control the formation of the $\alpha$-helix and $3_{10}$-helix remains an important subject in peptide chemistry. A number of experimental studies have shown the conversion between different secondary structures for polypeptides in the gas phase.[2−14] On the other hand, many theoretical calculations have been reported on the energies and conformations of small- and medium-sized polypeptides[15−36] or infinitely long peptides using periodic models.[14,37−39] It has been generally accepted that with respect to the $\beta$-strand structures (without HBs) both $\alpha$- and $3_{10}$-helical structures exhibit significant amounts of cooperativity.[26−30,33,38,40] The cooperative interaction in both helical structures is suggested to originate from the additive electrostatic interaction and some nonadditive short-range many-body effects (such as the induction energy). For example, Wu and Zhao have investigated the formation of $\alpha$-helix and $3_{10}$-helix for a series of polyglycines up to 14 residues at the Hartree−Fock (HF) and B3LYP[41−43] density functional theory levels. They found that the long-range electrostatic interaction among residues is mainly responsible for the cooperative effects in the $\alpha$-helix and $3_{10}$-helix conformations.[26,27] Wieczorek and Dannenberg[28−32] have obtained the optimized structures and energies of $\alpha$-helices, $3_{10}$-helices, and $\beta$-strands for small and medium-sized capped polyalanines, acetyl(ala)$_N$NH$_2$ ($N$ = 2−18), with the B3LYP and ONIOM(B3LYP:AM1) methods. They found that in the gas phase the $3_{10}$-helices are more stable than the isomeric $\alpha$-helices for all polyalanines up to $N = 18$, but $\alpha$-helices may become more stable for larger values of $N$. Their analyses also indicated that in both helices the nonadditive component of the energetic cooperativity is very important. Baker et al. studied the origin of HB cooperativity in $\alpha$-helices and found that the long-range electrostatic interaction among residues and short-range nonadditive many-body effects make roughly equal contributions to HB cooperativity.[33] Yang et al. studied the relative stability of $\alpha$- and $3_{10}$-helical structures for short peptides (acetyl-(ala)$_N$-methylamide, $N$ = 2, 3, 5, 8) with B3LYP and the van der Waals (vdW) corrected B3LYP, B3LYP(vdW).[35,36] They found that the energy difference between $3_{10}$-helix and $\alpha$-helix drops dramatically when the empirical vdW energy term is added to the B3LYP energy. They further conjectured that the $\alpha$-helix will become more stable in long chain peptides (than the corresponding $3_{10}$-helix) due to the stronger vdW interaction. Very recently (during the revision of the present work), Scheffler et al.[39] calculated the capped polyalanines up to 20 residues and an infinite periodic chain at the ideal $\alpha$-helical and $3_{10}$-helical geometries with the vdW-corrected density functional theory (DFT). They showed that the inclusion of vdW interaction greatly enhances not only the relative stability of helical structures with respect to the fully extended structure but also the relative stability of the $\alpha$-helix with respect to the $3_{10}$-helix.

Up to now, most quantum mechanical calculations on polypeptides have been limited to small- or medium-sized peptides (the number of residues is usually less than 20). In recent years, we have developed a generalized energy-based fragmentation

**Received:** April 12, 2011
**Revised:** August 19, 2011
**Published:** August 22, 2011

approach (GEBF) for approximate quantum mechanical calculations of very large molecules,[44] and other groups have developed similar approaches.[45−51] The basic idea of the GEBF approach is that the ground-state energy (or energy derivative) of a large molecule can be approximately evaluated as the linear combination of the energies (or energy derivatives) of a series of subsystems embedded in the presence of background point charges, which can be calculated with conventional quantum chemistry methods. The GEBF approach is applicable within various theoretical frameworks such as HF, DFT, and second-order perturbation theory (MP2), and it has been demonstrated to be quite accurate for various biological systems such as peptides and proteins.[52−54] In this work, we attempt to investigate the optimized structures, energies, and enthalpies of $\alpha$-helices, $3_{10}$-helices, and $\beta$-strands for capped polyalanines, acetyl-$(ala)_N NH_2$, up to 40 residues with the GEBF-DFT method. In comparison with GEBF-MP2 single-point energies, we find that the popular B3LYP functional used mostly in previous theoretical works on peptides is not reliable for estimating relative energies of different secondary structures in long polyalanines, while the recently developed M06-2X functional[55,56] can provide quite satisfactory results. Our results agree with the previous studies[55−58] that the M06-2X functional is quite reliable for accounting for van der Waals (vdW) interaction, which is not included in the B3LYP functional. Therefore, the M06-2X functional is adopted in this work. On the basis of the GEBF-M06-2X results, we will discuss the chain length dependence of the relative energies or enthalpies of $\alpha$-helices and $3_{10}$-helices (with respect to the $\beta$-strands). Special attention will be paid to revisit the origin and nature of the cooperative interaction in both helices and provide qualitative explanations on the relative order of cooperativity in $\alpha$-helices and $3_{10}$-helices. Our calculations reveal that both electrostatic and vdW interactions are essential in accounting for the cooperative interaction in long $\alpha$-helices and $3_{10}$-helices. This study presents clear evidence that the vdW interaction should be appropriately included in predicting the relative energies of various secondary structures in polypeptides.

## 2. COMPUTATIONAL DETAILS

The theoretical foundations and implementation details of the GEBF approach have been described in our previous work.[44,52−54,59−63] Here we only give a brief introduction on this approach. The main procedures of this approach include: (1) divide a large system into fragments of comparable size; (2) construct a series of subsystems from all fragments, according to some rules. A distance threshold ($\xi$) is used to control the size of subsystems (this is the only parameter used in GEBF for controlling its accuracy); (3) place each subsystem in the presence of background point charges generated by all atoms outside this subsystem; (4) perform conventional quantum chemistry calculations for all "embedded" subsystems; (5) obtain the total energy of the target molecule from the expression below,

$$E_{\mathrm{Tot}} = \sum_{m}^{M} C_m \tilde{E}_m - [(\sum_{m}^{M} C_m) - 1] \sum_{\mathrm{A}} \sum_{\mathrm{B>A}} \frac{Q_{\mathrm{A}} Q_{\mathrm{B}}}{R_{\mathrm{AB}}} \qquad (1)$$

where $\tilde{E}_m$ denotes the energy (including the self-energy of the point charges) of the $m$th subsystem, $C_m$ represent the coefficient of the $m$th subsystem ($M$ is the total number of subsystems), and $Q_{\mathrm{A}}$ represents the net charge on atom A. For neutral molecules without polar groups, one can assume that the net charge on every atom is zero, and thus the GEBF approach can reduce to the simpler energy-based fragmentation approach.[59]

Within the GEBF approach, the energy derivatives of the target system can also be evaluated easily. For example, the first- and second-derivatives of the total energy for a target system can be computed as below,

$$\frac{\partial E_{\mathrm{Tot}}}{\partial q_{Ii}} \approx \sum_{n} C_n \frac{\partial \tilde{E}_n}{\partial q_{Ii}} \qquad (2)$$

$$\frac{\partial E_{\mathrm{Tot}}}{\partial q_{Ii} \partial q_{Jj}} \approx \sum_{n} C_n \frac{\partial \tilde{E}_n}{\partial q_{Ii} \partial q_{Jj}} \qquad (3)$$

Here $q_{Ii}$ $(i = x, y, z)$ represents a certain Cartesian displacement of the $I$th atom, the summation over $n$ in eq 2 is limited to those subsystems containing atom $I$ as a real atom, and the summation in eq 3 includes those subsystems containing both atoms $I$ and $J$ as real atoms. Thus, the energy gradients and the energy Hessian of the target system can be assembled with the corresponding quantities of subsystems, which can be obtained with many ab initio packages. Our previous numerical calculations[54] have demonstrated that eqs 2 and 3 work well for a wide range of systems. With the energy gradients and the energy Hessian (obtained by using eqs 2 and 3), one can do geometry optimizations and vibrational frequency calculations for large molecules containing hundreds of atoms.

In this work, we take an alanine residue as a fragment for polyalanines and $\xi$ = 3.0 Å as the distance threshold for GEBF calculations. The largest subsystems in GEBF calculations only contain about 50−70 atoms and can be efficiently calculated by the conventional DFT or MP2 methods. For a given large system, the conventional calculations for all subsystems are carried out with the Gaussian 09 package,[64] and the total energy or energy derivatives are obtained with our own LSQC program.[65] With an interface between Gaussian 09 package and LSQC program, we apply the Berny algorithm in the Gaussian 09 package to perform GEBF geometry optimizations at various levels of theory. At GEBF-optimized geometries, we perform vibrational frequency calculations with the LSQC program to verify whether they are minimum structures and to obtain the thermal corrections to enthalpies or free energies.

Let us describe how to add background point charges for each subsystem. These point charges are assumed to locate at the corresponding nuclear centers. For a given subsystem, all atoms beyond this subsystem including those junction atoms (atoms replaced by capping hydrogen atoms) are represented as point charges. In the first step, we perform conventional HF calculations on all primitive subsystems (without background point charges) to get an initial guess for net atomic charges on all atoms. Next, a conventional HF calculation is carried out again for each primitive subsystem, which is placed into the background point charges generated above, and more realistic net atomic charges can be obtained. We have found that the natural atomic charges from the first iteration are nearly convergent. A detailed description on this procedure has been discussed in our previous work.[44,54]

The accuracy of the GEBF approach for systems under study is validated by comparing the optimized geometries and their energies obtained with conventional DFT and GEBF-DFT calculations for acetyl$(ala)_{10}NH_2$ with the 6-31G** basis set. The results are shown in Table S1 in the Supporting Information.

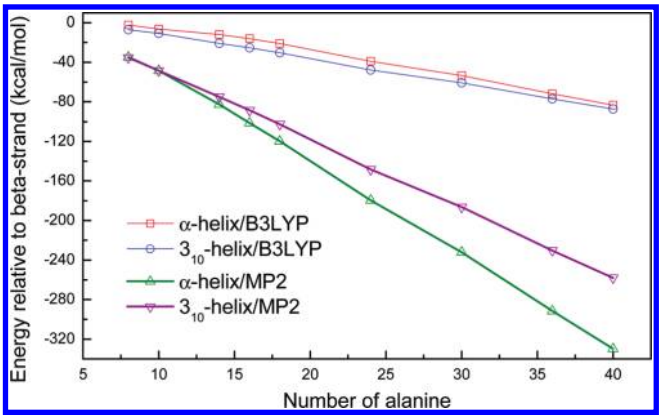


**Figure 1.** Relative energies of $\alpha$-helices and $3_{10}$-helices (with respect to the energy of the respective $\beta$-strand) obtained with GEBF-B3LYP/6-311++G** and GEBF-MP2/6-311++G** calculations at the geometries optimized by GEBF-B3LYP/6-31G**.

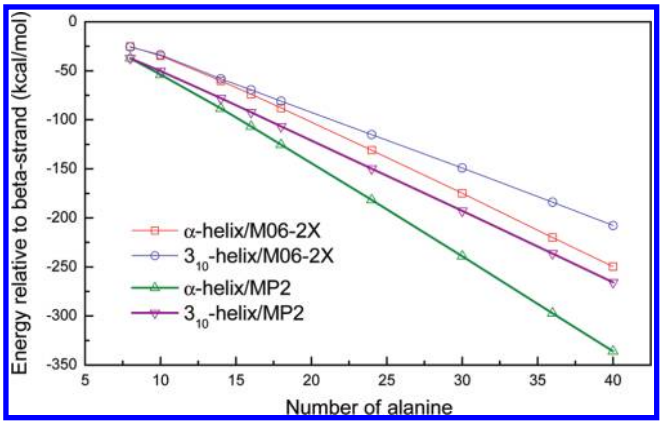


**Figure 2.** Relative energies of $\alpha$-helices and $3_{10}$-helices (with respect to the energy of the respective $\beta$-strand) obtained with GEBF-M06-2X/6-311++G** and GEBF-MP2/6-311++G** calculations at the geometries optimized by GEBF-M06-2X/6-31G**.

From Table S1, one can see that the root-mean-square distance (rmsd) between the optimized structures from GEBF-DFT and conventional DFT calculations is less than 0.14 Å, and the energy difference is less than 3 millihartree (mH) for both B3LYP and M06-2X functionals. Thus, the GEBF-DFT approach is expected to reproduce accurate energies and geometries as the conventional DFT approach for all polyalanines under study.

## 3. RESULTS AND DISCUSSION

In this section, the GEBF approach will be employed to investigate the structures, energies, and enthalpies of $\alpha$-helices, $3_{10}$-helices, and $\beta$-strands for capped polyalanines up to 40 residues. For convenience in later discussions, we will use the nomenclature $\alpha(N)$, $3_{10}(N)$, and $\beta(N)$ to represent the corresponding structures with $N$-alanines. First, the performance of two DFT functionals, B3LYP and M06-2X, for the systems under study will be evaluated by comparing the relative energies of $\alpha(N)$ and $3_{10}(N)$ ($N$ = 8, 10, 14, 16, 18, 24, 30, 36, 40) obtained with GEBF-DFT and GEBF-MP2 calculations. Our calculations show that the M06-2X functional is much more accurate than the B3LYP functional for systems under study. Then, on the basis of the GEBF-M06-2X results, the relative stability of the two helices and their dependence on the chain length will be compared. In the last subsection, we will give detailed discussions to analyze the nature and origin of the cooperative interaction in both helices and provide a qualitative picture on understanding the relative order of cooperativity in $\alpha$-helices and $3_{10}$-helices.

**3.1. Performance of B3LYP and M06-2X Functionals.** To determine which functional is more appropriate for peptides under study, we first apply the GEBF-B3LYP and GEBF-M06-2X methods with the 6-31G** basis set to fully optimize the structures of $\alpha(N)$, $3_{10}(N)$, and $\beta(N)$ for $N$ = 8−40. Then, at optimized geometries obtained with the B3LYP or M06-2X functional, we carry out single-point GEBF-DFT and GEBF-MP2 calculations with a larger 6-311++G** basis set. The relative energies of $\alpha(N)$ and $3_{10}(N)$ (relative to the energies of $\beta(N)$) for a series of $N$ values) obtained with two different methods are collected in Tables S2 and S3 of the Supporting Information and displayed in Figures 1 and 2, respectively. It can be seen from Figure 1 that the relative energies calculated by GEBF-B3LYP are very different from those calculated by GEBF-MP2. The GEBF-B3LYP results show that $\alpha$-helices are always less stable than the corresponding $3_{10}$-helices, while the GEBF-MP2 results predict the reverse trend (except for $N$ = 8, 10). However, the relative stability order of $\alpha(N)$ and $3_{10}(N)$ predicted by GEBF-M06-2X agrees reasonably well with that predicted by GEBF-MP2. At GEBF-M06-2X geometries, both GEBF-M06-2X and GEBF-MP2 approaches predict that $\alpha(N)$ is more stable than $3_{10}(N)$ for $N \geq 10$. For $N$ = 8, the $\alpha$-helix is predicted to be identical in energy to the $3_{10}$-helix by GEBF-MP2, but slightly higher in energy than the $3_{10}$-helix by GEBF-M06-2X (as shown in Table S3 of the Supporting Information). It should be pointed out that MP2 is not a benchmark method for peptides under study. For both helices their relative energies from GEBF-MP2 calculations are somewhat larger in magnitude than those from GEBF-M06-2X calculations. This discrepancy is probably due to the overestimation of the MP2 method for the dispersion interaction energy.[66,67] Nevertheless, the MP2 method is still qualitatively correct for the peptides under study.[68,69] In summary, the M06-2X functional is a better choice than the B3LYP functional for systems under study. The main difference between the M06-2X and B3LYP functionals can be ascribed to the better treatment of medium-range exchange-correlation energy and the inclusion of dispersion-like interactions.[55−59,70−75] Thus, in the next subsection, only M06-2X results will be used to discuss the relative stabilities of $\alpha$-helices and $3_{10}$-helices for different $N$ values.

To validate whether the 6-31G** basis set is adequate for geometry optimizations of peptides under study, we also carry out geometry optimizations with a large basis set, 6-31+G**, for $\alpha(N)$, $3_{10}(N)$, and $\beta(N)$ with $N$ = 10 and 16. Then, at optimized geometries obtained with GEBF-M06-2X/6-31+G**, we perform single-point GEBF-M06-2X calculations with the 6-311++G** basis set. One can see from Table S4 of the Supporting Information that for $N$ = 10 and 16 the relative energies of $\alpha(N)$ and $3_{10}(N)$ (relative to $\beta(N)$) calculated at the GEBF-M06-2X/6-31+G** geometries agree well with the corresponding values calculated at the GEBF-M06-2X/6-31G** geometries (the differences are less than 1.3 kcal/mol). Hence, the 6-31G** basis set is demonstrated to be adequate for geometry optimizations of the peptides.

We also carry out single point calculations with a larger cc-pVTZ basis set to verify whether the qualitative trend obtained with the 6-311++G** basis set remains true for polypeptides

Table 1. Average HB Lengths (in Å) in $\alpha$-Helices and $3_{10}$-Helices of Acetyl(ala)$_N$NH$_2$ ($N$ = 8−40)[a]

| $N$ | GEBF-M06-2X[b] | | GEBF-B3LYP[b] | |
|---|---|---|---|---|
| | $\alpha$-helix | $3_{10}$-helix | $\alpha$-helix | $3_{10}$-helix |
| 8 | 2.20 (8) | 2.02 (7) | 2.19 (7) | 2.11 (7) |
| 10 | 2.15 (10) | 2.00 (9) | 2.18 (9) | 2.10 (9) |
| 14 | 2.09 (14) | 1.98 (13) | 2.15 (14) | 2.07 (13) |
| 16 | 2.07 (16) | 1.98 (15) | 2.16 (16) | 2.06 (15) |
| 18 | 2.06 (18) | 1.98 (17) | 2.14 (18) | 2.06 (17) |
| 24 | 2.03 (24) | 1.96 (23) | 2.10 (24) | 2.04 (23) |
| 30 | 2.01 (30) | 1.96 (29) | 2.08 (30) | 2.04 (29) |
| 36 | 2.00 (36) | 1.96 (35) | 2.06 (36) | 2.03 (35) |
| 40 | 1.99 (40) | 1.95 (39) | 2.05 (40) | 2.03 (39) |

[a] The geometries are optimized with GEBF-M06-2X and GEBF-B3LYP at the 6-31G** level. [b] The number of HBs is included in parentheses.

Table 2. Average N−H···O Angles (in Degrees) for HBs in $\alpha$-Helices and $3_{10}$-Helices of Acetyl(ala)$_N$NH$_2$ ($N$ = 8−40)[a]

| $N$ | GEBF-M06-2X | | GEBF-B3LYP | |
|---|---|---|---|---|
| | $\alpha$-helix | $3_{10}$-helix | $\alpha$-helix | $3_{10}$-helix |
| 8 | 148.3 | 166.1 | 157.4 | 167.3 |
| 10 | 149.6 | 166.2 | 160.4 | 167.3 |
| 14 | 151.7 | 166.0 | 155.1 | 167.4 |
| 16 | 152.3 | 165.3 | 155.5 | 167.2 |
| 18 | 152.5 | 165.0 | 156.1 | 166.6 |
| 24 | 153.5 | 165.0 | 157.4 | 166.8 |
| 30 | 154.1 | 163.5 | 158.2 | 166.1 |
| 36 | 154.6 | 163.5 | 158.5 | 166.3 |
| 40 | 154.6 | 164.3 | 158.9 | 167.2 |

[a] The geometries are optimized with GEBF-M06-2X and GEBF-B3LYP at the 6-31G** level.

Table 3. Relative Energies of $\alpha(N)$ and $3_{10}(N)$ ($N$ = 8−40) Relative to Those of $\beta(N)$ Obtained with M06-2X, B3LYP, and B3LYP(vdW) Functionals at the 6-311++G** Level[a]

| $n$ | GEBF-M06-2X | | GEBF-B3LYP | | GEBF-B3LYP(vdW[b]) | |
|---|---|---|---|---|---|---|
| | $\alpha$-helix | $3_{10}$-helix | $\alpha$-helix | $3_{10}$-helix | $\alpha$-helix | $3_{10}$-helix |
| 8 | −25.2 | −25.7 | 6.9 | −5.4 | −20.6 | −26.6 |
| 10 | −34.6 | −33.9 | 6.6 | −8.9 | −31.1 | −37.2 |
| 14 | −60.4 | −58.1 | 1.2 | −17.7 | −57.0 | −60.7 |
| 16 | −73.9 | −69.3 | −2.0 | −22.1 | −71.0 | −72.9 |
| 18 | −87.8 | −80.8 | −4.9 | −26.8 | −84.8 | −85.0 |
| 24 | −130.9 | −115.0 | −16.3 | −40.4 | −129.0 | −122.3 |
| 30 | −174.8 | −149.2 | −28.6 | −53.6 | −173.0 | −158.1 |
| 36 | −219.9 | −184.0 | −40.8 | −67.0 | −216.6 | −193.1 |
| 40 | −249.7 | −207.7 | −49.0 | −77.7 | −246.5 | −218.5 |

[a] All calculations are done at the optimized geometries obtained with GEBF-M06-2X/6-31G**. [b] The vdW energy is evaluated with the empirical formula given in ref 36.

under study. Some recent studies showed that intramolecular basis set superposition error (BSSE) can significantly affect the energy differences between various conformers of large systems.[76−78] With the cc-pVTZ basis set, the effect of intramolecular BSSE on the relative energies of different conformers can be dramatically reduced.[78] One can see from Table S5 of the Supporting Information that, with the cc-pVTZ basis set, the relative energies of $\alpha(N)$ and $3_{10}(N)$ (relative to $\beta(N)$, $N$ = 8, 10, 14, 16) agree reasonably well with the corresponding values calculated with the 6-311++G** basis set (the differences are less than 4.2 kcal/mol for M06-2X and 2.1 kcal/mol for B3LYP). Although the cross point of the relative stability between $\alpha(N)$ and $3_{10}(N)$ is delayed from $N$ = 10 (M06-2X/6-311++G**) to $N$ = 14 (M06-2X/cc-pVTZ), the qualitative trend on the relative stability predicted with the cc-pVTZ basis set is consistent with that predicted by the 6-311++G** basis set.

Yang et al.[35,36] have performed constrained optimizations for acetyl-(ala)$_8$-methylamide with the B3LYP/6-31G* method and calculated the single point energies with the MP2/6-31G* method. Their results showed that for partially optimized $\alpha$-helix and $3_{10}$-helix (with standard $\phi$ and $\psi$ angles, but other freedoms are optimized) their energy difference is 2.6 kcal/mol at the MP2/6-31G* level and 6.2 kcal/mol at the B3LYP/6-31G* level. Thus, compared to MP2, B3LYP tends to underestimate the stability of the $\alpha$-helix (relative to the $3_{10}$-helix). Our results (shown in Table S2) show that this observation holds true for longer polypeptides.

**3.2. Structure of $\alpha$-Helices and $3_{10}$-Helices.** For $\alpha(N)$, $3_{10}(N)$, and $\beta(N)$ ($N$ = 8−40), we have optimized their structures with the GEBF-M06-2X approach with the 6-31G** basis set. It should be pointed out that, for all optimized $\alpha$-helices, the terminal residues at both C-terminus and N-terminus exist in a mixed $3_{10}/\alpha$-helical conformation (as shown in Figure S1 in the Supporting Information). At the C-terminus residue, its amide group forms an additional HB to the third alanine C═O. At the next terminal residue, the N−H group forms a normal HB to the fifth alanine and an additional HB to the fourth alanine. On the other hand, at the N-terminus, the terminal acetyl C═O forms a normal $\alpha$-helical HB to the fourth alanine N−H and an additional HB to the third alanine. The mixed $3_{10}/\alpha$-helical character of the terminal residues does not change when the length of peptides increases. Since the number of HBs in the pure $\alpha$-helices of acetyl(ala)$_N$NH$_2$ is $N$ − 3, the total number of HBs is $N$ for all optimized $\alpha$-helices ($N \geq 10$). For $3_{10}(N)$, each structure is a pure $3_{10}$-helix, which contains $(N-1)$ HBs. For both $\alpha(N)$ and $3_{10}(N)$, the average HB lengths are listed in Table 1. One can see that for both $\alpha$-helices and $3_{10}$-helices the average HB length decreases as $N$ increases. However, for $\alpha(N)$ or $3_{10}(N)$ the average HB length gradually approaches a constant value when $N$ is sufficiently large. This constant value may be around 1.99 Å for infinite $\alpha$-helices or 1.95 Å for infinite $3_{10}$-helices. In general, the average HB length of $\alpha$-helices is somewhat longer than that of the corresponding $3_{10}$-helices.[30,37,79] On the other hand, the average N−H···O angles for HBs are listed in Table 2. One can see that the average N−H···O angle in $\alpha$-helices increases slightly as $N$ increases, but that in $3_{10}$-helices decreases slightly as $N$ increases.

For the purpose of comparison, we have also obtained the optimized structures of $\alpha(N)$ and $3_{10}(N)$ ($N$ = 8−40) at the GEBF-B3LYP/6-31G** level. These structures are very similar to those obtained with GEBF-M06-2X calculations. However, for the same helical structure the average HB length calculated with GEBF-B3LYP (also collected in Table 1) is significantly longer than that calculated with GEBF-M06-2X (except for $N$ = 8). The difference between average HB lengths obtained with M06-2X

**Table 4. Relative Enthalpies, Relative Enthalpies per Residue, and Relative Enthalpies per Hydrogen Bond of $\alpha(N)$ and $3_{10}(N)$ ($N$ = 8−40) Relative to Those of $\beta(N)$[a]**

| | $\Delta H$ | | $\Delta H/N_{ala}$ | | $\Delta H/n_{HB}$[b] | |
|---|---|---|---|---|---|---|
| $N$ | $\alpha$-helix | $3_{10}$-helix | $\alpha$-helix | $3_{10}$-helix | $\alpha$-helix | $3_{10}$-helix |
| 8 | −24.6 | −24.7 | −3.1 | −3.1 | −3.1 | −3.5 |
| 10 | −33.7 | −32.6 | −3.4 | −3.3 | −3.4 | −3.6 |
| 14 | −58.7 | −56.6 | −4.2 | −4.0 | −4.2 | −4.4 |
| 16 | −71.1 | −66.7 | −4.4 | −4.2 | −4.4 | −4.4 |
| 18 | −84.2 | −77.5 | −4.7 | −4.3 | −4.7 | −4.6 |
| 24 | −127.1 | −111.5 | −5.3 | −4.6 | −5.3 | −4.8 |
| 30 | −169.6 | −144.3 | −5.7 | −4.8 | −5.7 | −5.0 |
| 36 | −220.6 | −185.8 | −6.1 | −5.2 | −6.1 | −5.3 |
| 40 | −247.8 | −207.4 | −6.2 | −5.2 | −6.2 | −5.3 |

[a] ZPVEs and thermal corrections at 298 K are obtained with GEBF-M06-2X/6-31G**, and electronic energies are obtained with GEBF-M06-2X/6-311++G** at the GEBF-M06-2X/6-31G** geometries. [b] The number of HBs for each structure is listed in Table 1.

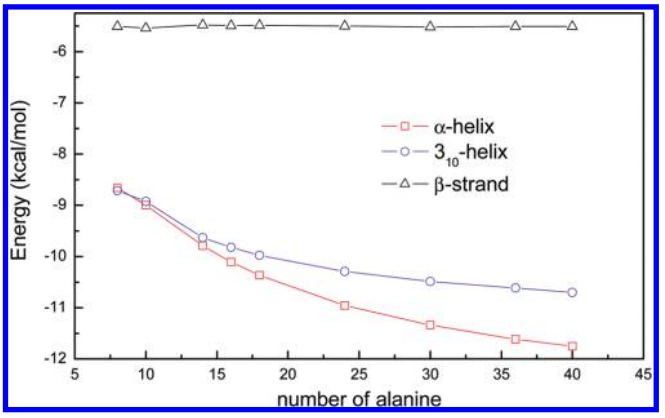


**Figure 3.** Polymerization energies per alanine for $\alpha$-helices, $3_{10}$-helices, and $\beta$-strands obtained with GEBF-M06-2X/6-311++G** at the geometries optimized by GEBF-M06-2X/6-31G**.

and B3LYP functionals reflects that the dispersion-like interaction may play an important role in enhancing the hydrogen bond strengths in longer helices.

**3.3. Relative Stabilities of $\alpha$-Helices and $3_{10}$-Helices.** To compare the relative stabilities of $\alpha$-helices and $3_{10}$-helices, we have performed single-point GEBF-M06-2X calculations with the 6-311++G** basis set for $\alpha(N)$, $3_{10}(N)$, and $\beta(N)$ ($N$ = 8−40) at the GEBF-M06-2X/6-31G** geometries. The relative energies of $\alpha(N)$ and $3_{10}(N)$ with respective to the $\beta$-strand counterpart are shown in Table 3. One can see that $\alpha$-helices are more stable than the corresponding $3_{10}$-helices for $N \geq 10$, and as the number of alanines increases, the relative energies of $\alpha$-helices decrease more steeply than those of $3_{10}$-helices. For example, $\alpha(10)$ is lower in energy than $3_{10}(10)$ by about 0.7 kcal/mol, but $\alpha(40)$ is lower than $3_{10}(40)$ by 42.0 kcal/mol. On the other hand, by combining the GEBF-M06-2X/6-311++G** electronic energies with zero-point vibrational energies and thermal corrections at 298 K calculated at the GEBF-M06-2X/6-31G** level, we have also obtained the relative enthalpies of $\alpha(N)$ and $3_{10}(N)$ (with respective to the $\beta$-strand counterpart), as shown in Table 4. One can see that relative

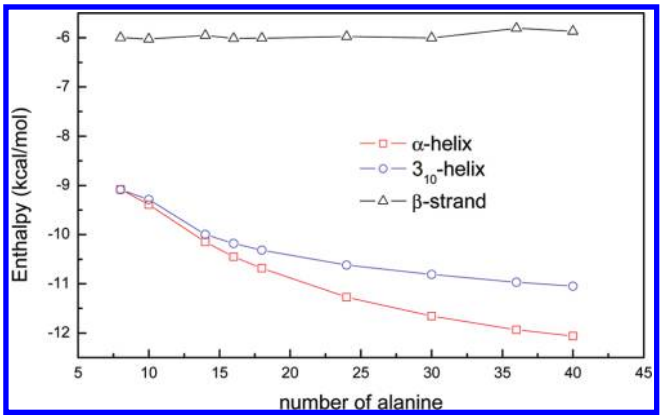


**Figure 4.** Polymerization enthalpies per alanine for $\alpha$-helices, $3_{10}$-helices, and $\beta$-strands obtained with GEBF-M06-2X/6-311++G** at the geometries optimized by GEBF-M06-2X/6-31G**.

enthalpies of both helices are similar to their relative energies in magnitude. The reason for this result is that vibrational corrections for three secondary structures are almost the same. The data in Table 4 also show that the enthalpic stability per alanine ($\Delta H/N_{ala}$) or that per hydrogen bond of both helices over the strand continues to increase in magnitude as $N$ increases. The relative enthalpies per alanine of both helices obtained here are dramatically larger in magnitude than those estimated previously.[31] We will discuss this discrepancy later. A rough extrapolation of the curves for both helices suggests that the relative enthalpy per alanine will approach −7.8 kcal/mol in $\alpha$-helices and −5.8 kcal/mol in $3_{10}$-helices, respectively, when the peptide becomes much longer.

It is interesting to relate the energies or enthalpies of capped polyalanines to the number of alanines using the following condensation reaction proposed previously,[30]

$$N\text{-}alanines + CH_3COOH + NH_3 \rightarrow \text{acetyl(ala)}_N NH_2 + (N+1)H_2O \quad (4)$$

The polymerization energy (or enthalpy) of the capped polypeptide is defined as the energy (or enthalpy) change of the above reaction. The polymerization energies or enthalpies per alanine for $\alpha(N)$, $3_{10}(N)$, and $\beta(N)$ as a function of $N$ are presented in Figures 3 and 4, respectively. One can see that the polymerization energies (or enthalpies) per alanine for $\beta$-strands keeps almost constant as $N$ increases, but those of $\alpha$-helices and $3_{10}$-helices show downward curvatures. This result suggests that the polymerization energies of $\beta$-strands can be evaluated using a group additivity relationship, but those of both helices exhibit significant amounts of cooperativity. Since the downward curvature is greater for $\alpha$-helices than $3_{10}$-helices, the cooperativity is stronger in $\alpha$-helices than that in $3_{10}$-helices.

**3.4. Origin of Cooperativity in $\alpha$-Helices and $3_{10}$-Helices.** The nature and origin of cooperativity in helical structures of polypeptides have been analyzed in a number of previous works.[26−30,33,37,38] The fact that the polymerization energies (or enthalpies) of $\alpha$-helices and $3_{10}$-helices become more negative as the number of alanines increases is a clear indication of cooperativity. In addition, changes in physical properties of polyalanines with increasing the chain length also indicate cooperativity in $\alpha$-helices and $3_{10}$-helices. For example, as shown in the preceding subsection, the average HB length in both $\alpha$-helices and $3_{10}$-helices decreases as $N$ increases. For three kinds of secondary

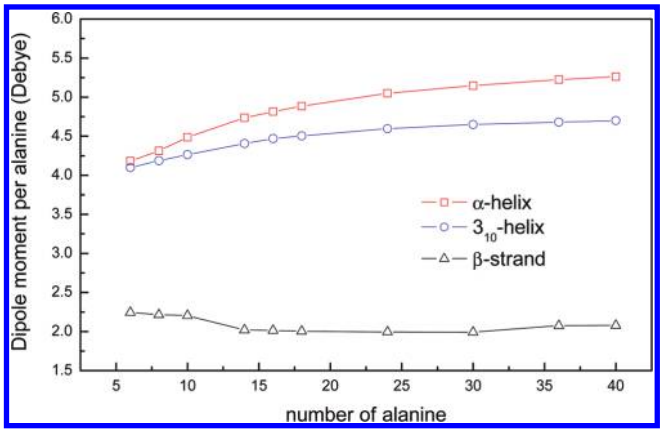


**Figure 5.** Dipole moments per alanine for $\alpha$-helices, $3_{10}$-helices, and $\beta$-strands obtained with GEBF-M06-2X/6-31G** at GEBF-M06-2X/6-31G** geometries.

structures, the dependence of their dipole moments per alanine on the chain length is displayed in Figure 5. It can be seen that the dipole moments per alanine in $\beta$-strands keep almost constant, but those in both helices continue to increase as the peptide grows. The increasing trend in $\alpha$-helices is noticeably greater than that in $3_{10}$-helices. By analyzing the optimized GEBF-M06-2X/6-31G** geometries of two helices, we find that intrahelical hydrogen bonds in $\alpha$-helices are aligned more parallel to the helical axis than those in $3_{10}$-helices. The results here are similar to those obtained previously for short polyalanines ($N \leq 18$).[30,37]

To analyze the components of the cooperative interaction in both helices, we have performed single-point GEBF-B3LYP/6-311++G** calculations for three secondary structures at their GEBF-M06-2X/6-31G** geometries. The results are also shown in Table 3 for comparison. Surprisingly, one can see the dramatic differences between M06-2X and B3LYP results. The GEBF-B3LYP results predict that $\alpha$-helices are less stable than $3_{10}$-helices for all polyalanines under study. As described earlier, the difference between M06-2X and B3LYP results may be partially ascribed to the contribution of the vdW interaction to the stability and cooperativity of both helices. Clearly, the vdW interaction energy tends to stabilize both helices over the $\beta$-strand counterparts. For example, for $N = 40$ the relative energy of $3_{10}(N)$ (relative to $\beta(N)$) is $-77.7$ kcal/mol at the B3LYP level, but $-207.7$ kcal/mol at the M06-2X level. The energy difference, $-130.0$ kcal/mol, may be considered to be largely from the vdW interaction. Considering the fact that the B3LYP functional works reasonably well for hydrogen bonding interactions,[80] one may conclude that both electrostatic and vdW interaction are responsible for the cooperative interaction in both helices. On the other hand, with the empirical expression given by Wu and Yang[36] we have also calculated the vdW corrections at M06-2X-optimized geometries for three different conformers of polyalanines ($N = 8-40$). The results collected in Table 3 also indicate that the B3LYP(vdW) energies are in good agreement with the M06-2X results. The similarity between B3LYP(vdW) and M06-2X results indicates that for systems under study the difference between M06-2X and B3LYP is mostly from the inclusion of the dispersion-like interactions in M06-2X.

The cooperative interaction in both helical structures is usually decomposed into pairwise interaction and nonpairwise interaction.[30,33] It is generally accepted that the pairwise interaction is due to the long-range electrostatic interaction and the nonpairwise interaction is due to the short-range many-body effects, which lead to shorter intrahelical hydrogen bonds in longer helices. However, one can see that for the same helical structure the average HB length in the M06-2X-optimized geometry is significantly shorter than that in the corresponding B3LYP-optimized geometry. Since the M06-2X function contains the vdW interaction, which is not included in the B3LYP functional, thus one may deduce that the vdW interaction can indeed result in enhanced hydrogen bonding.

**Table 5. Backbone Lengths (in Å) of Polyalanines at Optimized Structures Obtained with GEBF-M06-2X/6-31G**[a]**

| $N$ | $\alpha$-helix | $3_{10}$-helix | $\beta$-strand | $N$ | $\alpha$-helix | $3_{10}$-helix | $\beta$-strand |
|---|---|---|---|---|---|---|---|
| 8 | 15.3 | 17.6 | 31.0 | 24 | 38.9 | 47.6 | 88.4 |
| 10 | 17.7 | 21.1 | 38.2 | 30 | 48.0 | 58.7 | 109.8 |
| 14 | 23.8 | 28.7 | 52.5 | 36 | 56.8 | 69.9 | 131.1 |
| 16 | 27.1 | 32.2 | 59.6 | 40 | 62.8 | 77.7 | 145.4 |
| 18 | 29.6 | 35.9 | 66.6 | | | | |

[a] Here the backbone length is defined as the longest distance between two terminal non-hydrogen atoms.

We should also mention that the long-range electrostatic interaction is certainly another factor for enhancing hydrogen bonds in longer helical structures. As shown in optimized structures obtained at the GEBF-B3LYP/6-31G** level, the average HB length in both $\alpha$-helices and $3_{10}$-helices decreases gradually as the system size increases. Since the B3LYP functional performs well for hydrogen-bonding interactions, this fact indicates that the long-range electrostatic interaction also contributes to the increased hydrogen bond strengths in longer helices.

From the discussions above, we conclude that the cooperative interaction in longer helical structures is due to both electrostatic and vdW interactions. Both interactions are very important in stabilizing helices over the corresponding $\beta$-strands. Our calculations also suggest that the electrostatic and vdW interactions can indirectly lead to shorter hydrogen bonds and greater dipole moments (per residue) in longer helices. These effects were considered as two indicators of short-range nonpairwise (or nonadditive) cooperative interactions. Hence, our conclusion here is quite different from the generally accepted viewpoint that the cooperative interaction in long helices is mainly from the long-range electrostatic interaction and the short-range many-body effects. The reason why the present study leads to different conclusions from previous studies is that only the HF and B3LYP methods were employed in most of previous theoretical calculations.[26−31] Due to the neglect of the vdW interaction, the relative energies or enthalpies per alanine of both helices reported previously[31] are much smaller than those we obtain in the present work. We should mention that the existence of the nonadditive component of the energetic cooperativity cannot be ruled out. Several effects such as polarizability, charge transfer, and covalent interaction (between donors and acceptors of HBs) might also result in structural distortions in longer helices.[30] Nevertheless, these effects are difficult to be rationally quantified, and we conjecture that these nonadditive interactions are much less important than the electrostatic and van der Waals interactions.

As shown in Tables 3 and 4, the cooperativity in $\alpha$-helices is stronger than that in $3_{10}$-helices. It might be interesting to provide a qualitative explanation for this result. By comparing the relative energies of $\alpha$-helices and $3_{10}$-helices (relative to the

$\beta$-strands) obtained with GEBF-B3LYP/6-311++G** calculations, one can find that $3_{10}$-helices are always much more stable than the corresponding $\alpha$-helices. In general, the B3LYP method can treat the long-range electrostatic interaction reasonably well. Hence, one may infer that the long-range electrostatic interaction is more favorable in $3_{10}$-helices rather than in $\alpha$-helices. This result is in contradiction with the viewpoint that the long-range electrostatic interaction stabilizes $\alpha$-helices over $3_{10}$-helices.[28−33] A comparison of GEBF-M06-2X relative energies with GEBF-B3LYP results (Table 3) clearly shows that the vdW interaction plays a dominant role in stabilizing $\alpha$-helices over $3_{10}$-helices in longer helices ($N \geq 10$), which is consistent with the result from a recent study.[39] By checking the lengths of the polypeptide backbone in optimized structures obtained with GEBF-M06-2X (Table 5), we find that $\alpha$-helices are always shorter than $3_{10}$-helices, and both helices are much shorter than $\beta$-strands for all $N$ values. For example, the backbone length is 62.8, 77.7, 145.4 Å in $\alpha(40)$, $3_{10}(40)$, and $\beta(40)$, respectively. Hence, the structures of $\alpha$-helices are more spatially crowded than those of $3_{10}$-helices, which lead to stronger dispersion-like interactions in $\alpha$-helices.

## 4. CONCLUSIONS

In this work, we have employed the GEBF approach to investigate the structures, energies, and enthalpies of $\alpha$-helices, $3_{10}$-helices, and $\beta$-strands for capped polyalanines up to 40 residues at several theoretical levels. We show that the M06-2X functional is much more accurate than the B3LYP functional for peptides under study. On the basis of the GEBF-M06-2X results, we have found that $\alpha$-helices are more stable than the corresponding $3_{10}$-helices for all $N$ values (except $N = 8$), which is consistent with the result from a recent study.[39] The energetic cooperativities of both helices over the reference $\beta$-strands have not reached their asymptotic limits even for $N = 40$. By comparing the results of the M06-2X and B3LYP functionals, we present clear evidence that the cooperative interaction in long $\alpha$-helices and $3_{10}$-helices is mainly due to both electrostatic and vdW interactions. This observation is in sharp contrast to the generally accepted viewpoint that the cooperative interaction in long helices is from the long-range electrostatic interaction and the short-range many-body effects.[28−33] Our calculations suggest that shorter hydrogen bonds and greater dipole moments (per residue) in long helices largely come from the indirect effect of the electrostatic and vdW interactions. On the other hand, the greater cooperativity of $\alpha$-helices over $3_{10}$-helices in long helices is found to mainly originate from the much stronger van der Waals interaction in $\alpha$-helices. A qualitative explanation for this result is that $\alpha$-helices are much more spatially crowded than $3_{10}$-helices, thus possessing stronger van der Waals interaction. This result is also different from the previously suggested viewpoint that the long-range electrostatic interaction stabilizes $\alpha$-helices over $3_{10}$-helices.

## ■ ASSOCIATED CONTENT

**Supporting Information.** Ground-state energies and relative energies with different calculation methods (Tables S1-S5) and optimization of the hydrogen bonds (Figure S1). This material is available free of charge via the Internet at http://pubs.acs.org.

## ■ AUTHOR INFORMATION

**Corresponding Author**
*E-mail: shuhua@nju.edu.cn.

## ■ ACKNOWLEDGMENT

This work was supported by the National Natural Science Foundation of China (Grant Nos. 21073086 and 20833003) and the National Basic Research Program (Grant No. 2011CB808501).

## ■ REFERENCES

(1) Creighton, T. E. *Proteins: Structures and Molecular Properties*, 2nd ed.; W. H. Freeman and Company: New York, 1993.
(2) Hudgins, R. R.; Ratner, M. A.; Jarrold, M. F. *J. Am. Chem. Soc.* **1998**, *120*, 12974.
(3) Jarrold, M. F. *Annu. Rev. Phys. Chem.* **2000**, *51*, 179.
(4) Lopez, M. M.; Chin, D. H.; Baldwin, R. L.; Makhatadze, G. I. *Proc. Natl. Acad. Sci. U.S.A.* **2002**, *99*, 1298.
(5) Shi, Z.; Olson, C. A.; Rose, G. D.; Baldwin, R. L.; Kallenbach, N. R. *Proc. Natl. Acad. Sci. U.S.A.* **2002**, *99*, 9190.
(6) Kohtani, M.; Jones, T. C.; Schneider, J. E.; Jarrold, M. F. *J. Am. Chem. Soc.* **2004**, *126*, 7420.
(7) Sudha, R.; Kohtani, M.; Breaux, G. A.; Jarrold, M. F. *J. Am. Chem. Soc.* **2004**, *126*, 2777.
(8) Kohtani, M.; Jarrold, M. F. *J. Am. Chem. Soc.* **2004**, *126*, 8454.
(9) Chin, W.; Piuzzi, F.; Dognon, J.-P.; Dimicoli, I.; Tardivel, B.; Mons, M. *J. Am. Chem. Soc.* **2005**, *127*, 11900.
(10) Hatakeyama, Y.; Sawada, T.; Kawano, M.; Fujita, M. *Angew. Chem., Int. Ed.* **2009**, *48*, 8695.
(11) Jarrold, M. F. *Phys. Chem. Chem. Phys.* **2007**, *9*, 1659.
(12) Kinnear, B. S.; Kaleta, D. T.; Kohtani, M.; Hudgins, R. R.; Jarrold, M. F. *J. Am. Chem. Soc.* **2000**, *122*, 9243.
(13) Kubelka, J.; Gangani, R. A.; Silva, D.; Keiderling, T. A. *J. Am. Chem. Soc.* **2002**, *124*, 5325.
(14) Rossi, M.; Blum, V.; Kupser, P.; Helden, G. V.; Bierau, K. P.; Meijer, G.; Scheffler, M. *Phys. Chem. Lett.* **2010**, *1*, 3465.
(15) Zhang, L.; Hermans, J. *J. Am. Chem. Soc.* **1994**, *116*, 11915.
(16) Wang, Y.; Kuczera, K. *J. Phys. Chem. B* **1997**, *101*, 5205.
(17) Samuelson, S. O.; Martyna, G. J. *J. Phys. Chem. B* **1999**, *103*, 1752.
(18) Counterman, A. E.; Clemmer, D. E. *J. Phys. Chem. B* **2003**, *107*, 2111.
(19) Hudgins, R. R.; Jarrold, M. F. *J. Am. Chem. Soc.* **1999**, *121*, 3494.
(20) Kohtani, M.; Kinnear, B. S.; Jarrold, M. F. *J. Am. Chem. Soc.* **2000**, *122*, 12377.
(21) Elstner, M.; Jalkanen, K. J.; Knapp-Mohammady, M.; Frauenheim, T.; Suhai, S. *Chem. Phys.* **2000**, *256*, 15.
(22) Topol, I. A.; Burt, S. K.; Deretey, E.; Tang, T.-H.; Perczel, A.; Rashin, A.; Csizmadia, I. G. *J. Am. Chem. Soc.* **2001**, *123*, 6054.
(23) Bour, P.; Kubelka, J.; Keiderling, T. A. *Biopolymer* **2002**, *65*, 45.
(24) Ireta, J.; Neugebauer, J.; Scheffler, M.; Rojo, A.; Galván, M. *J. Am. Chem. Soc.* **2005**, *127*, 17241.
(25) Mándity, I. M.; Wéber, E.; Martinek, T. A.; Olajos, G.; Tóth, G. K.; Vass, E.; Fülöp, F. *Angew. Chem., Int. Ed.* **2009**, *48*, 2171.
(26) Zhao, Y.-L.; Wu, Y.-D. *J. Am. Chem. Soc.* **2002**, *124*, 1570.
(27) Wu, Y.-D.; Zhao, Y.-L. *J. Am. Chem. Soc.* **2001**, *123*, 5313.
(28) Kobko, N.; Dannenberg, J. J. *J. Phys. Chem. A* **2003**, *107*, 10389.
(29) Wieczorek, R.; Dannenberg, J. J. *J. Am. Chem. Soc.* **2003**, *125*, 8124.
(30) Wieczorek, R.; Dannenberg, J. J. *J. Am. Chem. Soc.* **2004**, *126*, 14198.
(31) Wieczorek, R.; Dannenberg, J. J. *J. Am. Chem. Soc.* **2005**, *127*, 14534.
(32) Tsai, M.; Xu, Y.; Dannenberg, J. J. *J. Phys. Chem. B* **2009**, *113*, 309.

(33) Morozov, A. V.; Tsemekhman, K.; Baker, D. *J. Phys. Chem. B* **2006**, *110*, 4503.
(34) Ismer, L.; Ireta, J.; Neugebauer, J. *J. Phys. Chem. B* **2008**, *112*, 4109.
(35) Liu, H.; Elstner, M.; Kaxiras, E.; Frauenheim, T.; Hermans, J.; Yang, W. *Proteins: Struct., Funct., Genet.* **2001**, *44*, 484.
(36) Wu, Q.; Yang, W. T. *J. Chem. Phys.* **2002**, *116*, 515.
(37) Improta, R.; Barone, V.; Kudin, K. N.; Scuseria, G. E. *J. Am. Chem. Soc.* **2001**, *123*, 3311.
(38) Ireta, J.; Neugebauer, J.; Scheffler, M.; Rojo, A.; Galván, M. *J. Phys. Chem. B* **2003**, *107*, 1432.
(39) Tkatchenko, A.; Rossi, M.; Blum, V.; Ireta, J.; Scheffler, M. *Phys. Rev. Lett.* **2011**, *106*, 118102.
(40) Koch, O.; Bocola, M.; Klebe, G. *Proteins: Struct., Funct., Bioinf.* **2005**, *61*, 310.
(41) Becke, A. D. *J. Chem. Phys.* **1993**, *98*, 5648.
(42) Becke, A. D. *Phys. Rev. A* **1988**, *38*, 3098.
(43) Lee, C.; Yang, W.; Parr, R. G. *Phys. Rev. B* **1988**, *37*, 785.
(44) Li, W.; Li, S.; Jiang, Y. *J. Phys. Chem. A* **2007**, *111*, 2193.
(45) Deev, V.; Collins, M. A. *J. Chem. Phys.* **2005**, *122*, 154102.
(46) Collins, M. A.; Deev, V. *J. Chem. Phys.* **2006**, *125*, 104104.
(47) Addicoat, M. A.; Collins, M. A. *J. Chem. Phys.* **2009**, *131*, 104103.
(48) Ganesh, V.; Dongare, R. K.; Balanarayan, P.; Gadre, S. R. *J. Chem. Phys.* **2006**, *125*, 104109.
(49) Deshmukh, M. M.; Gadre, S. R. *J. Phys. Chem. A* **2009**, *113*, 7927.
(50) Ahalkar, A. P.; Katouda, M.; Gadre, S. R.; Nagase, S. *J. Comput. Chem.* **2010**, *31*, 2405.
(51) Bettens, R. P. A.; Lee, A. M. *J. Phys. Chem. A* **2006**, *110*, 8777.
(52) Hua, W.; Fang, T.; Li, W.; Yu, J.; Li, S. *J. Phys. Chem. A* **2008**, *112*, 10864.
(53) Dong, H.; Hua, S.; Li, S. *J. Phys. Chem. A* **2009**, *113*, 1335.
(54) Hua, S.; Hua, W.; Li, S. *J. Phys. Chem. A* **2010**, *114*, 8126.
(55) Zhao, Y.; Truhlar, D. G. *Theor. Chem. Acc.* **2008**, *120*, 215.
(56) Zhao, Y.; Truhlar, D. G. *Acc. Chem. Res.* **2008**, *41*, 157.
(57) Tian, B.; Strid, Å.; Eriksson, L. A. *J. Phys. Chem. B* **2011**, *115*, 1918.
(58) Bertran, O.; Torras, J.; Alemán, C. *J. Phys. Chem. C* **2010**, *114*, 11074.
(59) Li, S.; Li, W.; Fang, T. *J. Am. Chem. Soc.* **2005**, *127*, 7215.
(60) Li, S.; Li, W. *Annu. Rep. Prog. Chem., Sect. C: Phys. Chem.* **2008**, *104*, 256.
(61) Li, W.; Dong, H.; Li, S. *Progress in Theoretical Chemistry and Physics*; Springer-Verlag: Berlin, 2008; Vol. 18, p 289.
(62) Li, W.; Hua, W.; Fang, T.; Li, S. *Computational Methods for Large Systems: Electronic Structure Approaches for Biotechnology and Nanotechnology*; Reimers, J. R., Ed.; John Wiley & Sons, Inc.: New York, 2011; p 227.
(63) Yang, Z.; Hua, S.; Hua, W.; Li, S. *J. Phys. Chem. A* **2010**, *114*, 9253.
(64) Frisch, M. J.; Trucks, G. W.; Schlegel, H. B.; Scuseria, G. E.; Robb, M. A.; Cheeseman, J. R.; Montgomery, J. A., Jr.; Vreven, T.; Kudin, K. N.; Burant, J. C.; Millam, J. M.; Iyengar, S. S.; Tomasi, J.; Barone, V.; Mennucci, B.; Cossi, M.; Scalmani, G.; Rega, N.; Petersson, G. A.; Nakatsuji, H.; Hada, M.; Ehara, M.; Toyota, K.; Fukuda, R.; Hasegawa, J.; Ishida, M.; Nakajima, T.; Honda, Y.; Kitao, O.; Nakai, H.; Klene, M.; Li, X.; Knox, J. E.; Hratchian, H. P.; Cross, J. B.; Adamo, C.; Jaramillo, J.; Gomperts, R.; Stratmann, R. E.; Yazyev, O.; Austin, A. J.; Cammi, R.; Pomelli, C.; Ochterski, J. W.; Ayala, P. Y.; Morokuma, K.; Voth, G. A.; Salvador, P.; Dannenberg, J. J.; Zakrzewski, V. G.; Dapprich, S.; Daniels, A. D.; Strain, M. C.; Farkas, O.; Malick, D. K.; Rabuck, A. D.; Raghavachari, K.; Foresman, J. B.; Ortiz, J. V.; Cui, Q.; Baboul, A. G.; Clifford, S.; Cioslowski, J.; Stefanov, B. B.; Liu, G.; Liashenko, A.; Piskorz, P.; Komaromi, I.; Martin, R. L.; Fox, D. J.; Keith, T.; Al-Laham, M. A.; Peng, C. Y.; Nanayakkara, A.; Challacombe, M.; Gill, P. M. W.; Johnson, B.; Chen, W.; Wong, M. W.; Gonzalez, C.; Pople, J. A. *Gaussian 09*, revision A.02; Gaussian, Inc.: Wallingford, CT, 2009.
(65) Li, S.; Li, W.; Fang, T.; Ma, J.; Hua, W.; Hua, S.; Jiang, Y. *Low-Scaling Quantum Chemistry (LSQC)*, Version 2.0; Nanjing University: Nanjing, 2010.
(66) Tkatchenko, A.; DiStasio, R. A.; Head-Gordon, M.; Scheffler, M. *J. Chem. Phys.* **2009**, *131*, 094106.
(67) Riley, K. E.; Pionak, M.; Jurecka, P.; Hobza, P. *Chem. Rev.* **2010**, *110*, 5023.
(68) Perczel, A.; Farkas, Ö.; Jákli, I.; Topol, I. A.; Csizmadia, I. G. *J. Comput. Chem.* **2003**, *24*, 1206.
(69) Bouteiller, Y.; Poully, J. C.; Desfrançois, C.; Grégoire, G. *J. Phys. Chem. A* **2009**, *113*, 6301.
(70) Riley, K. E.; Pionak, M.; Jurecka, P.; Hobza, P. *Chem. Rev.* **2010**, *110*, 5023.
(71) Steinmann, S. N.; Csonka, G.; Corminbouef, C. *J. Chem. Theory Comput.* **2009**, *5*, 2950.
(72) Johnson, E. R.; Mackie, I. D.; DiLabio, G. A. *J. Phys. Org. Chem.* **2009**, *22*, 1127.
(73) Hohenstein, E. G.; Chill, S. T.; Sherrill, C. D. *J. Chem. Theory Comput.* **2008**, *4*, 1996.
(74) Acosta-Silva, C.; Branchadell, V.; Bertran, J.; Oliva, A. *J. Phys. Chem. B* **2010**, *114*, 10217.
(75) Gloaguen, E.; de Courcy, B.; Piquemal, J.-P.; Pilme, J.; Parisel, O.; Pollet, R.; Biswal, H. S.; Piuzzi, F.; Tardivel, B.; Broquier, M.; Mons, M. *J. Am. Chem. Soc.* **2010**, *132*, 11861.
(76) Valdés, H.; Klusák, V.; Pitoňák, M.; Exner, O.; Starý, I.; Hobza, P.; Rulíšek, L. *J. Comput. Chem.* **2008**, *29*, 861.
(77) Adler, T. B.; Werner, H.-J. *J. Chem. Phys.* **2009**, *130*, 241101.
(78) Balabin, R. M. *Mol. Phys.* **2011**, *109*, 943.
(79) Voet, D.; Voet, J. G. *Biochemistry*, 2nd ed.; Wiley: New York, 1995.
(80) Improta, R.; Barone, V. *J. Comput. Chem.* **2004**, *25*, 1333.